Article

Cell Reports

Dual Regulation of Fbw7 Function and Oncogenic Transformation by Usp28

Graphical Abstract

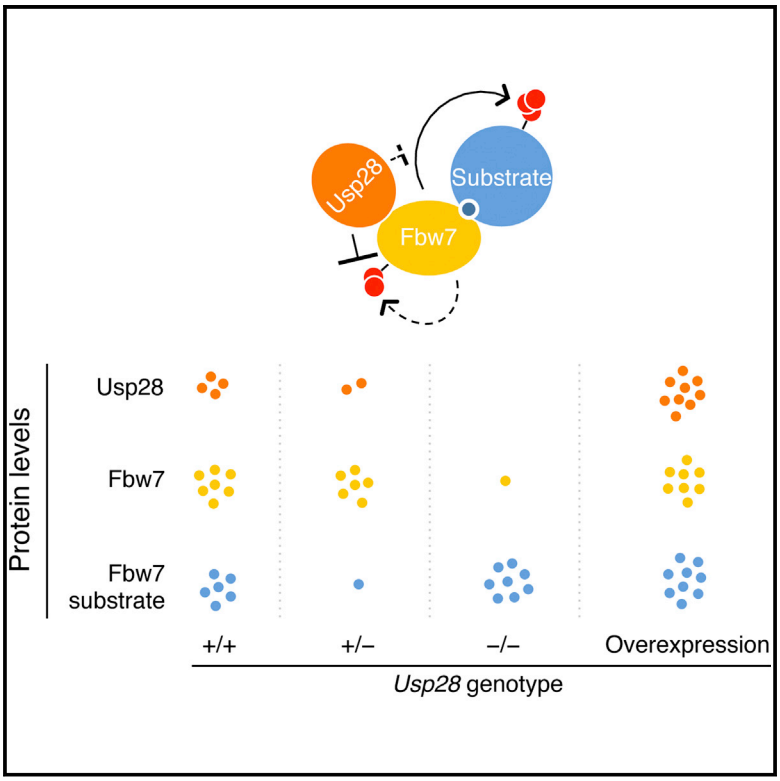

Authors

Christina Schülein-Völk, Elmar Wolf, ..., Martin Eilers, Nikita Popov

Correspondence

nikita.popov@biozentrum.uni-wuerzburg.de

In Brief

Schülein-Völk et al. show that the Usp28 deubiquitinase antagonizes both substrate targeting and autocatalytic ubiquitination by Fbw7 but preferentially deubiquitinates Fbw7. In mice, monoallelic loss of *Usp28* maintains stable Fbw7 but drives Fbw7 substrate degradation. Complete knockout of *Usp28* destabilizes Fbw7 and promotes Fbw7 substrate accumulation and Ras-driven oncogenic transformation.

Highlights

Usp28 deubiquitinates and stabilizes Fbw7

Complete knockout of *Usp28* promotes autoubiquitination and degradation of Fbw7

Overexpression of Usp28 stabilizes both Fbw7 and its substrates

Complete loss and overexpression of *Usp28* promote oncogenic transformation

Accession Numbers

GSE59354

Schülein-Völk et al., 2014, Cell Reports 9, 1099–1109
November 6, 2014 ©2014 The Authors
http://dx.doi.org/10.1016/j.celrep.2014.09.057

Cell Reports
Article

Dual Regulation of Fbw7 Function and Oncogenic Transformation by Usp28

Christina Schülein-Völk,[1] Elmar Wolf,[1] Jing Zhu,[2] Wenshan Xu,[2] Lyudmyla Taranets,[2] Andreas Hellmann,[2] Laura A. Jänicke,[1] Markus E. Diefenbacher,[3] Axel Behrens,[3] Martin Eilers,[1,2] and Nikita Popov[1,2,*]
[1]Department of Biochemistry and Molecular Biology, Biozentrum, University of Würzburg, Am Hubland, 97074 Würzburg, Germany
[2]Comprehensive Cancer Center Mainfranken and Department of Radiation Oncology, University Hospital Würzburg, Versbacher Strasse 5, 97078 Würzburg, Germany
[3]Mammalian Genetics Laboratory, Cancer Research UK London Research Institute, Lincoln's Inn Fields Laboratories 44, Lincoln's Inn Fields, London WC2A 3LY, UK
*Correspondence: nikita.popov@biozentrum.uni-wuerzburg.de
http://dx.doi.org/10.1016/j.celrep.2014.09.057

SUMMARY

Fbw7, the substrate recognition subunit of SCF(Fbw7) ubiquitin ligase, mediates the turnover of multiple proto-oncoproteins and promotes its own degradation. Fbw7-dependent substrate ubiquitination is antagonized by the Usp28 deubiquitinase. Here, we show that Usp28 preferentially antagonizes autocatalytic ubiquitination and stabilizes Fbw7, resulting in dose-dependent effects in *Usp28* knockout mice. Monoallelic deletion of *Usp28* maintains stable Fbw7 but drives Fbw7 substrate degradation. In contrast, complete knockout triggers Fbw7 degradation and leads to the accumulation of Fbw7 substrates in several tissues and embryonic fibroblasts. On the other hand, overexpression of Usp28 stabilizes both Fbw7 and its substrates. Consequently, both complete loss and ectopic expression of Usp28 promote Ras-driven oncogenic transformation. We propose that dual regulation of Fbw7 activity by Usp28 is a safeguard mechanism for maintaining physiological levels of proto-oncogenic Fbw7 substrates, which is equivalently disrupted by loss or overexpression of Usp28.

INTRODUCTION

Molecular mechanisms mediating protein degradation are essential for homeostasis and are frequently deregulated in human malignancies (Hoeller and Dikic, 2009). A prominent example is Fbw7 (hCdc4), which encodes the substrate recognition subunit of an SCF (Skp1-Cullin1-F-box) ubiquitin ligase (Welcker and Clurman, 2008). Fbw7 controls the abundance of a large number of proto-oncoproteins, including Myc, cyclin E, Jun, and NICD (Notch intracellular domain). Tissue-specific ablation of Fbw7 in mice typically results in increased proliferation and impaired differentiation of stem cells, resulting in strong homeostatic defects (Wang et al., 2012). Fbw7 is deregulated in approximately 10% of all human cancers, usually by point mutations, which compromise substrate binding and lead to inefficient ubiquitination (Akhoondi et al., 2007). The resulting increase in the levels of substrates like Myc, Mcl1, and cyclin E is thought to drive proliferation, attenuate apoptosis, and induce genomic instability, ultimately promoting tumorigenesis (Wang et al., 2012).

Fbw7-mediated substrate turnover is controlled at several levels. Degradation of individual substrates is mediated by phosphorylation at the conserved Fbw7 recognition motif, the Cdc4 phospho-degron (CPD). For example, Myc is phosphorylated at CPD by MAPK and Gsk3 kinases, whereas cyclin E requires phosphorylation by Gsk3 and Cdk2 (Welcker and Clurman, 2008).

In contrast, posttranslational modifications of Fbw7 may simultaneously modulate its activity toward multiple substrates. For instance, phosphorylation of the nucleoplasmic isoform of Fbw7 at Ser10 and Ser18 controls its subcellular localization and, potentially, degradation of several compartment-specific substrates (Durgan and Parker, 2010). Phosphorylation also regulates the turnover of Fbw7, which is largely mediated by autocatalytic ubiquitination (Min et al., 2012; Welcker et al., 2013). For example, phosphorylation at Ser227 downstream of PI3K enhances Fbw7 activity toward Myc, cyclin E, and Notch but attenuates its own turnover (Mo et al., 2011; Schülein et al., 2011). Similarly, phosphorylation at Ser205 leads to the recruitment of Pin1 peptidyl-prolyl isomerase, which attenuates substrate ubiquitination but promotes autocatalytic ubiquitin transfer (Min et al., 2012).

Degradation of several Fbw7 substrates, including Myc, Jun, and HIF1a is reversed by the Usp28 deubiquitinase (Popov et al., 2007a; Flügel et al., 2012; Diefenbacher et al., 2014). In unstressed cells, Usp28 forms a complex with Fbw7 and antagonizes substrate ubiquitination, whereas after DNA damage this complex dissociates, promoting Fbw7-dependent substrate degradation (Popov et al., 2007b). Usp28 is overexpressed in human colorectal cancer and deletion of *Usp28* attenuates Apc^{min}-driven intestinal tumorigenesis in mice, demonstrating that Usp28 acts as a tumor promoter in the intestine (Diefenbacher et al., 2014). Usp28 also stabilizes multiple proteins in the DNA damage response pathways, including 53BP1 and Claspin, but is dispensable for physiological DNA repair in vivo (Zhang et al., 2006; Bassermann et al., 2008; Knobel et al., 2014).

Here, we show that in mice Usp28 controls Fbw7 activity in a dose-dependent and tissue-specific manner. Whereas monoallelic deletion uniformly downregulates Fbw7 substrates, complete loss of Usp28, unexpectedly, rescues Fbw7 substrate levels in multiple tissues and embryonic fibroblasts. We show that partial loss of Usp28 maintains stable Fbw7 but promotes Fbw7 substrate degradation due to preferential deubiquitination of Fbw7 by Usp28. In contrast, complete absence of Usp28 induces Pin1-dependent autocatalytic ubiquitination and turnover of Fbw7 and leads to the accumulation of Fbw7 substrates. Thus, our data identify Usp28 as a bifunctional context-specific regulator of Fbw7 function.

RESULTS

Usp28 Controls Fbw7 Substrates in a Tissue-Specific and Dose-Dependent Manner

To study the impact of Usp28 on Fbw7 substrate turnover in vivo, we have generated conditional knockout mice (Diefenbacher et al., 2014). To obtain *Usp28*$^{+/-}$ mice, we crossed *Usp28*$^{fl/fl}$ mice with *Zp3-cre* mice, which express Cre recombinase in oocytes (de Vries et al., 2000). Intercrossing of *Usp28*$^{+/-}$ mice produced offspring at the expected Mendelian ratios; littermates of different genotypes were similar in appearance and weight (Figure S1A). Adult *Usp28*$^{-/-}$ mice appeared healthy and were fertile, had a normal lifespan, and did not develop spontaneous tumors. They produced offspring at the expected ratios demonstrating that long-term deficiency of Usp28 does not strongly affect embryonic development or reproductive function.

In tumor cell lines, Usp28 controls stability of Myc by antagonizing SCF(Fbw7) (Popov et al., 2007a). To test whether this mechanism operates in vivo, we examined levels of Myc in tissues of mice with different levels of *Usp28*. In the intestine and cerebellum, Myc levels gradually declined with loss of one and two alleles of *Usp28* (Figure 1A). Strikingly, in other analyzed tissues Myc levels declined in the *Usp28*$^{+/-}$ tissues but matched or exceeded the wild-type levels in the complete absence of *Usp28* (Figure 1A). *Myc* mRNA did not parallel protein levels, suggesting that Usp28 controls Myc abundance via posttranscriptional mechanisms in vivo (Figure S1B).

Importantly, loss of Usp28 synchronously deregulated multiple Fbw7 substrates. In small intestine, Jun, mTOR, cyclin E, Mcl1, and NICD, similar to Myc, gradually declined with loss of *Usp28* (Figure 1B). On the contrary, in the lung, these proteins showed biphasic pattern of regulation, decreasing in *Usp28*$^{+/-}$ mice and remaining at wild-type levels or accumulating in *Usp28*$^{-/-}$ mice. Acute deletion of *Usp28* in adult *Usp28*$^{fl/fl}$, *Rosa26-creER* mice by intraperitoneal injections of tamoxifen also reduced Fbw7 substrate levels in the intestine but had no effect or led to their accumulation in the lung, demonstrating that the effects on Fbw7 substrates in *Usp28* germline knockout mice are direct and not due to developmental compensation (Figure S1C).

Next, we tested whether this regulation was preserved in mouse embryonic fibroblasts (MEFs) with different genetic status of *Usp28*. Primary *Usp28*$^{+/-}$ MEFs presented flattened and enlarged morphology and showed a marked decrease in proliferation rate compared to wild-type MEFs. In contrast, primary *Usp28*$^{-/-}$ MEFs had normal morphology and proliferated even more efficiently than the *Usp28*$^{+/+}$ MEFs (Figures S1D and S1E). *Usp28*$^{+/-}$ fibroblasts underwent senescence earlier than *Usp28*$^{+/+}$ or *Usp28*$^{-/-}$ MEFs, as judged by β-galactosidase staining and upregulation of p19ARF, p53, and CDK inhibitors p16 and p21 (Figures S1E and S1F).

Immortalized *Usp28*$^{+/-}$ MEFs also displayed flattened and enlarged morphology and had a significant proliferative defect, compared to wild-type and *Usp28*$^{-/-}$ MEFs, as shown by colony formation assays and cumulative cell counting after serial replating (Figures 1C and 1D). These features were accompanied by a significant attenuation of DNA synthesis in *Usp28*$^{+/-}$ MEFs as determined by bromodeoxyuridine (BrdU) incorporation (Figure 1E). Importantly, Fbw7 substrate levels followed the pattern observed in most of the analyzed murine tissues, with a sharp decrease in the *Usp28*$^{+/-}$ and no change or an increase in the *Usp28*$^{-/-}$ MEFs (Figure 1F). The levels of encoding mRNAs changed only moderately with the exception of *Myc*, which was strongly upregulated in the *Usp28*$^{+/-}$ cells, in agreement with the finding that Myc represses transcription of its own mRNA (Figure S1G) (Penn et al., 1990).

We concluded that Usp28 regulates the abundance of Fbw7 substrates at a posttranscriptional step in a tissue-specific and dose-dependent manner.

Monoallelic Deletion of *Usp28* Destabilizes Fbw7 Substrates

To determine whether deregulation of Fbw7 substrates in *Usp28*-knockout cells occurs at the level of protein degradation, we incubated MEFs with the proteasome inhibitor, MG132. Upon treatment, levels of Myc, Jun, Mcl1, and mTOR became equivalent in cells with different status of Usp28 (Figure 2A). Interestingly, absolute levels of Usp28 and Mcl1 proteins did not increase in this experiment, likely due to the downregulation of the encoding mRNAs (Figure S2A). Levels of NICD were only partially rescued by proteasome inhibition, suggesting that additional mechanisms contribute to the downregulation of NICD in *Usp28*$^{+/-}$ cells (Figure 2A).

Analysis of protein levels after treatment with cycloheximide, a protein synthesis inhibitor, revealed that the turnover of Myc, NICD, Jun, Mcl1, and mTOR was strongly accelerated in *Usp28*$^{+/-}$ MEFs compared to wild-type and *Usp28*$^{-/-}$ MEFs (Figures 2B and S2B). In contrast, monoallelic loss of *Usp28* did not destabilize cyclins D1 and D2, which are degraded independently of Fbw7 (Figures 2B and S2B) (Vaites et al., 2011; Chen et al., 2012).

To test whether enhanced protein turnover upon monoallelic loss of *Usp28* is mediated by Fbw7, we made use of a cancer-derived Fbw7 mutant, R465H, which acts in a dominant-negative manner, possibly by sequestering wild-type Fbw7 in inactive dimers (Akhoondi et al., 2007; Welcker and Clurman, 2008). Ectopic expression of mutant Fbw7 rescued abundance of several Fbw7 substrates, including Myc, Jun, and mTOR (Figure 2C) in the *Usp28*$^{+/-}$ MEFs. Similar to the effects of proteasome inhibition, expression of NICD was only partially rescued by mutant Fbw7. Likewise, Fbw7 depletion with two independent small hairpin RNAs (shRNAs) rescued levels of Myc, Jun,

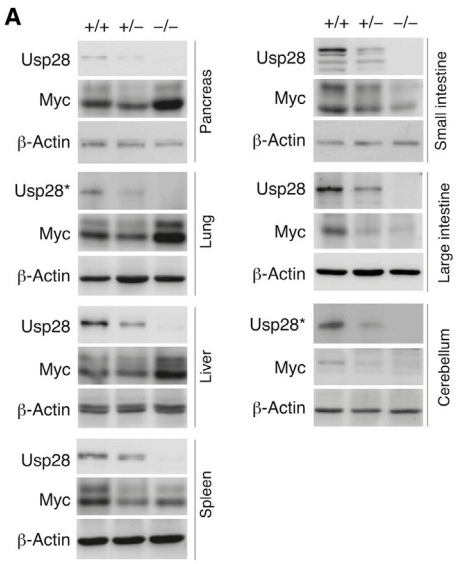

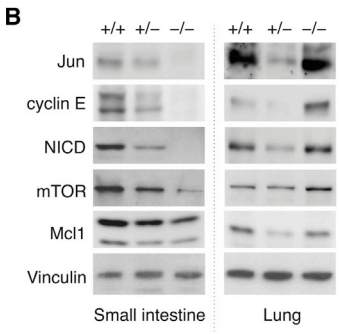

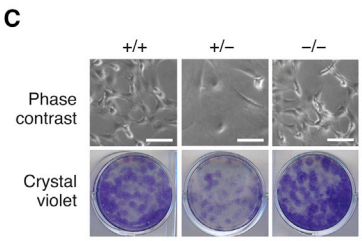

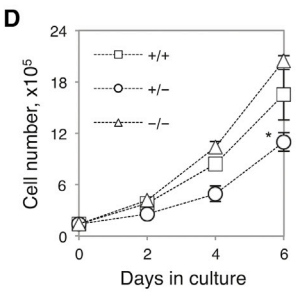

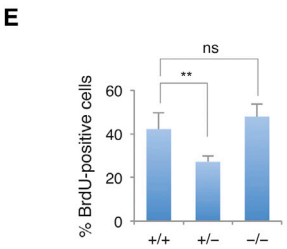

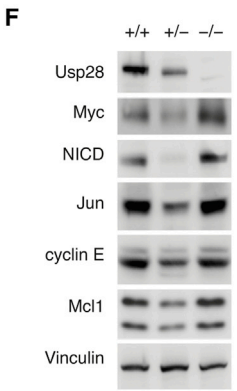

Figure 1. Usp28 Regulates Fbw7 Substrates in a Dose-Dependent and Tissue-Specific Manner

(A) Tissue lysates from mice with different levels of Usp28 were analyzed for expression of Myc by immunoblotting. For lung and cerebellum, Usp28 was immunoprecipitated prior to immunoblotting. A representative experiment from the analysis of three sets of mice is shown. See also Figures S1B and S1C.

(B) Lysates of small intestine and lung used in (A) were analyzed for the expression of indicated Fbw7 substrates by immunoblotting.

(C) Phase-contrast images of MEFs with different levels of *Usp28*, immortalized using shRNA vectors targeting *Arf* (upper panel). Scale bar, 100 μm. Lower panel shows crystal-violet-stained colonies of wild-type or Usp28 knockout MEFs. A representative image of three experiments is shown.

(D) Cumulative growth curve for MEFs with different status of *Usp28*. Equal cell numbers were replated and counted every 2 days. Error bars show SD. Cell numbers of Usp28 knockout MEFs at the last time point were compared to the number of wild-type MEFs using two-tailed Student's t test, *p = 0.04.

(E) Subconfluent MEF cultures were labeled with BrdU, fixed, stained with anti-BrdU antibody and propidium iodide, and analyzed by fluorescence-activated cell sorting. Error bars show SD of four biological replicates. The values were compared using Student's t test, **p = 0.009.

(F) Immunoblots documenting protein levels of Fbw7 substrates in immortal MEFs of the noted genotypes. A representative image of three MEF preparations is shown.

and mTOR but not of NICD, in *Usp28*$^{+/-}$ MEFs (Figures S2C and S2D; data not shown). Furthermore, expression of dominant-negative Fbw7 or Fbw7-targeting shRNAs enhanced proliferation of *Usp28*$^{+/-}$ MEFs, suggesting that their proliferative defect is, at least in part, mediated by the activated proteolysis of Fbw7 substrates (Figures 2D and S2E).

Taken together, these observations demonstrate that partial loss of *Usp28* profoundly enhances degradation of multiple Fbw7 substrates, implicating Usp28 as a general modulator of Fbw7 activity.

Complete Loss of *Usp28* Promotes Autocatalytic Degradation of Fbw7

Next, we sought to determine the molecular mechanisms responsible for Fbw7 substrate stabilization upon complete loss of Usp28. We considered the possibility that a component of the SCF(Fbw7) ubiquitin ligase is unstable in the *Usp28*-null cells, compromising ubiquitin conjugation. Deletion of *Usp28* did not affect levels of Cul1, Rbx1, or Cdc34 (the cognate ubiquitin-conjugating enzyme for SCF[Fbw7]), and slightly decreased levels of Skp1 (Figure 3A). Intriguingly, levels of Fbw7 did not change significantly in *Usp28*$^{+/-}$ MEFs but were strongly downregulated in *Usp28*$^{-/-}$ MEFs, with modest effects on the encoding mRNA (Figures 3A and S3A). Complete loss of Usp28 also led to a pronounced decrease in Fbw7 levels in murine tissues, which showed a biphasic effect on Fbw7 substrate abundance in lung, liver, and pancreas (Figure 3B, compare to Figures 1A and 1B). In contrast, Fbw7 was not significantly downregulated in the intestine and cerebellum of *Usp28*$^{-/-}$ mice, inversely correlating with levels of Fbw7 substrates in these tissues. Knockdown of Usp28 in human tumor

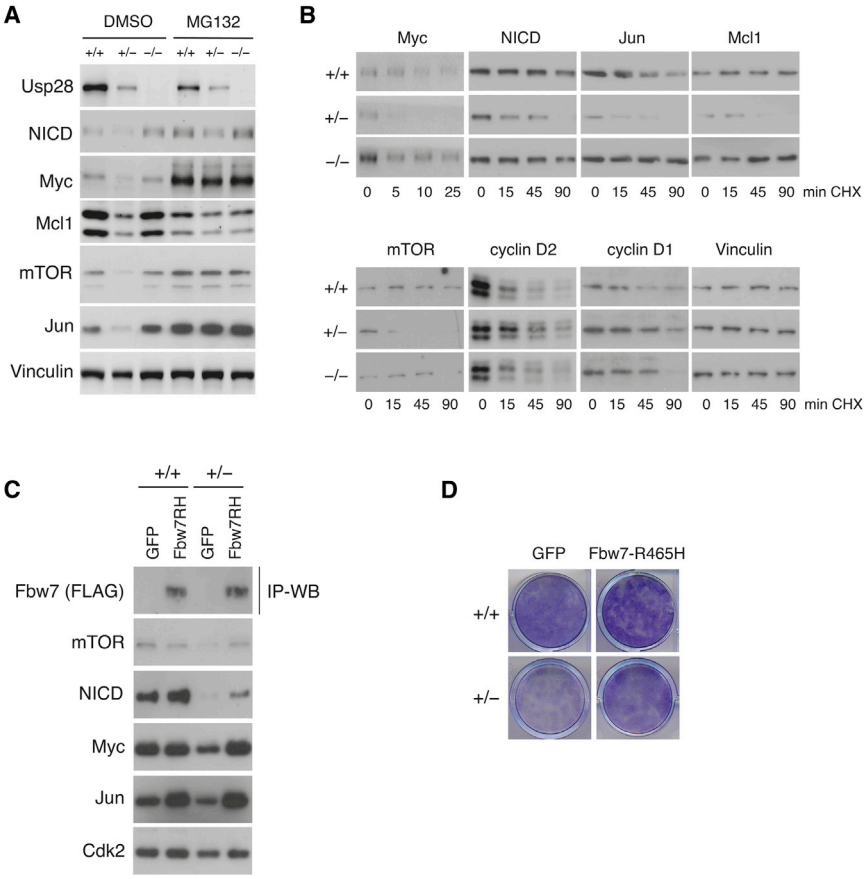

Figure 2. Monoallelic Loss of *Usp28* Destabilizes Fbw7 Substrates

(A) MEFs were treated with MG132 or DMSO for 8 hr and whole-cell lysates were analyzed by immunoblotting. The experiment was performed three times with similar results. See Figure S2A for mRNA levels of *Usp28* and *Mcl1*.

(B) MEFs were cultured in the presence of cycloheximide for the indicated time. Total cell lysates were analyzed by immunoblotting. See Figure S2B for quantification.

(C) *Usp28*$^{+/+}$ and *Usp28*$^{+/-}$ MEFs were transduced with retroviruses expressing R465H mutant Fbw7 or GFP; cell extracts were analyzed by immunoblotting. The result is representative of two independent experiments. See also Figure S2C.

(D) Crystal-violet-stained colonies of *Usp28*$^{+/+}$ and *Usp28*$^{+/-}$ MEFs expressing GFP or Fbw7 R465H mutant.

cells also decreased endogenous Fbw7 levels, suggesting that regulation by Usp28 is a conserved mechanism that maintains Fbw7 stability (Figure S3B).

Steady-state levels of Fbw7 in *Usp28*$^{-/-}$ MEFs were rescued by MG132 treatment, demonstrating that Fbw7 was degraded by the proteasome in the absence of Usp28 (Figure 3C). Cycloheximide chase experiments confirmed that complete loss of Usp28 strongly destabilized endogenous or ectopically expressed Fbw7 (Figures 3D, 3E, S3C, and S3D), whereas monoallelic loss did not have a major impact on Fbw7 degradation. Importantly, mutation of the F-box motif, which prevents incorporation of Fbw7 into the SCF complex, fully rescued Fbw7 stability in the *Usp28*-null MEFs, arguing that turnover of Fbw7 in the absence of Usp28 is mediated by autocatalytic ubiquitin transfer (Figures 3E and S3D) (Min et al., 2012; Welcker et al., 2013).

Autocatalytic ubiquitination by Fbw7 is regulated by several posttranslational modifications, including phosphorylation at Ser205 and subsequent isomerization by Pin1 (Min et al., 2012). We reasoned that modulation of this pathway might revert enhanced degradation of Fbw7 in the absence of Usp28 and promote substrate turnover. In agreement with this hypothesis, treatment of *Usp28*$^{-/-}$ MEFs with PiB, a specific Pin1 inhibitor, attenuated degradation of ectopic Fbw7 (Figures 3F and S3E). Similarly, Fbw7 turnover was delayed by mutation of Ser205, a phospho-acceptor site, required for Pin1 binding (Figures 3F and S3E). Stable expression of the S205A mutant Fbw7, but not of the wild-type protein, strongly downregulated Fbw7 substrates and attenuated proliferation of the *Usp28*$^{-/-}$ MEFs (Figures 3G and S3F). Likewise, treatment with Pin1 inhibitor rescued degradation of endogenous Fbw7 and downregulated Fbw7 substrates in *Usp28*$^{-/-}$ MEFs (Figure 3H). In contrast, PiB treatment did not significantly affect Fbw7 substrate levels in wild-type or *Usp28*$^{+/-}$ MEFs, suggesting that Usp28 balances effects of Pin1 on Fbw7-mediated ubiquitination (Figure 3H). Consistent with the effects on Fbw7 substrates, Pin1 inhibition attenuated proliferation of *Usp28*-null MEFs, but had little effect on the proliferation of *Usp28*$^{+/+}$ or *Usp28*$^{+/-}$ MEFs (Figure S3G). Moreover, expression of Pin1 correlated with Fbw7 substrate abundance in murine tissues; it decreased upon Usp28 loss in the intestine but increased in the lung, suggesting that tissue-specific regulation of Pin1 underlies the differential impact of Usp28 deletion on Fbw7 substrates (Figure S3H).

Thus, complete loss of Usp28 promotes Pin1-dependent degradation of Fbw7 by the proteasome, most likely via enhanced autocatalytic ubiquitination.

Usp28 Stabilizes Fbw7 and Its Substrates at Distinct Abundance Thresholds

Destabilization of Fbw7 in *Usp28*$^{-/-}$ cells suggested that Fbw7 is a substrate of Usp28, consistent with the efficient interaction between these two proteins (Popov et al., 2007a). Indeed, wild-type Usp28, but not the catalytically inactive C171A mutant, promoted Fbw7 deubiquitination in vivo (Figure 4A).

To test whether Usp28 directly deubiquitinates Fbw7, we used an in vitro assay with immunopurified SCF(Fbw7) and recombinant E1 and E2 enzymes, which leads to the accumulation of autoubiquitinated Fbw7 (Figure 4B) (Welcker et al., 2013). Addition of immunopurified wild-type Usp28, but not of the catalytic

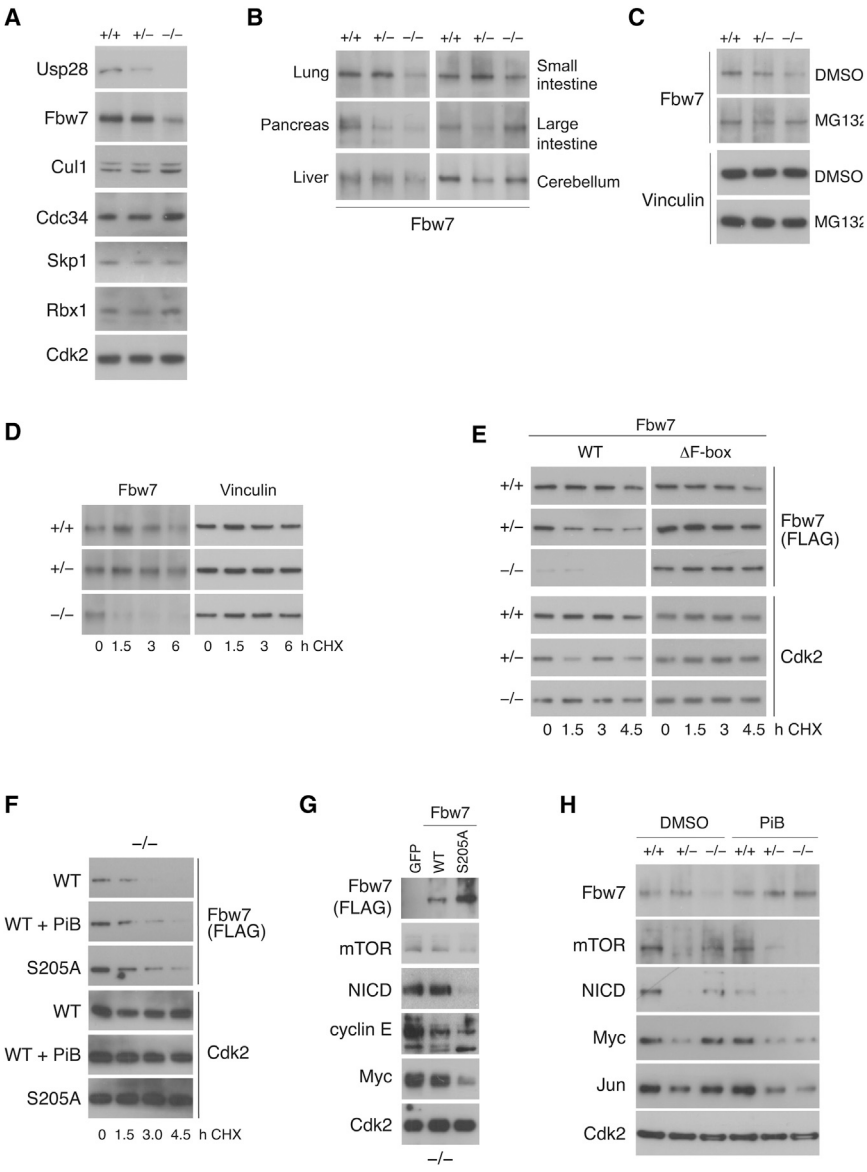

Figure 3. Complete Loss of *Usp28* Promotes Autocatalytic Degradation of Fbw7

(A) Immortal MEFs with different status of Usp28 were analyzed by immunoprecipitation (for Fbw7) and/or immunoblotting. A representative image of three experiments is shown. See Figure S3A for *Fbxw7* mRNA levels.

(B) Endogenous Fbw7 protein levels in mouse tissue samples shown in Figure 1A, analyzed by immunoprecipitation with A301-720A antibody followed by immunoblotting with 3B6 antibody (see Supplemental Experimental Procedures). This analysis was performed on a single set of tissue samples.

(C) MEFs were treated with MG132 for 12 hr; cell extracts were immunoprecipitated and immunoblotted with Fbw7 antibody. A representative of three experiments is shown.

(D) MEFs were treated with cylcoheximide for the indicated time, collected, and analyzed by immunoprecipiation and immunoblotting. A representative of three experiments is shown. See Figure S3C for quantification.

(E) MEFs were transiently transfected with wild-type Fbw7 or ΔF-box-Fbw7 expression constructs and incubated with cycloheximide for the indicated times. Cell lysates were analyzed by immunoblotting. A representative of three experiments is shown. See Figure S4D for quantification.

(F) Cycloheximide-treated *Usp28*$^{-/-}$ MEFs transfected with vectors encoding wild-type Fbw7 or the S205A mutant and preincubated with PiB (20 μM) or DMSO for 24 hr were analyzed by immunoblotting. See Figure S4E for quantification.

(G) Wild-type or S205A mutant FLAG-tagged Fbw7 were stably expressed in *Usp28*$^{-/-}$ MEFs by retroviral transduction, and cell extracts were analyzed Fbw7 substrates by immunoprecipitation and/or immunoblotting.

(H) MEFs treated with 20 μM PiB or DMSO for 48 hr were analyzed for the expression of Fbw7 and its substrates by immunoprecipitation and/or immunoblotting. A representative of three experiments is shown.

mutant, efficiently deubiquitinated Fbw7, demonstrating that Usp28 removes chains assembled by SCF(Fbw7) in an autocatalytic reaction (Figure 4B). Consistent with these observations, loss of Usp28 led to the accumulation of ubiquitinated endogenous Fbw7 in murine fibroblasts and tissues as well as in human tumor cells (Figures 4C and S4A).

To understand the nature of the nonlinear relationship between Usp28 and Fbw7 substrate abundance in murine tissues and cultured cells, we tested the sensitivity of ubiquitinated Fbw7 versus an Fbw7 substrate (Myc) to Usp28. We transfected HeLa cells with FLAG-tagged Myc or Fbw7 together with HA-tagged ubiquitin and increasing amounts of Usp28 and recovered ubiquitinated proteins by immunoprecipitation. Interestingly, Fbw7 was deubiquitinated already at the lowest level of Usp28, whereas Myc deubiquitination required significantly higher levels of the enzyme (Figure 4D).

To determine the consequences of such differential activity of Usp28, we cotransfected Fbw7 substrates (Figure 4E, lane 1), together with Fbw7 (lane 2), and increasing amounts of Usp28 (lanes 3-6). Fbw7 was stabilized in response to a minimal dose of cotransfected Usp28, whereas efficient stabilization of Myc, NICD, Mcl1, and mTOR occurred only at higher levels of Usp28 (Figure 4E). Importantly, this result was replicated in *Usp28*-null MEFs with tetracycline-inducible expression of Usp28; Fbw7 substrates were downregulated at low level of induced Usp28 but recovered at higher levels of Usp28 (Figure S4B). To test if the biphasic regulation of Fbw7 substrates by Usp28 is conserved in human cells, we generated clones of HeLa cells stably expressing different shRNA vectors against Usp28 resulting in a variable degree of knockdown. Similar to the situation in MEFs, Myc, cyclin E, Jun, and mTOR were strongly downregulated in clones with moderate depletion of

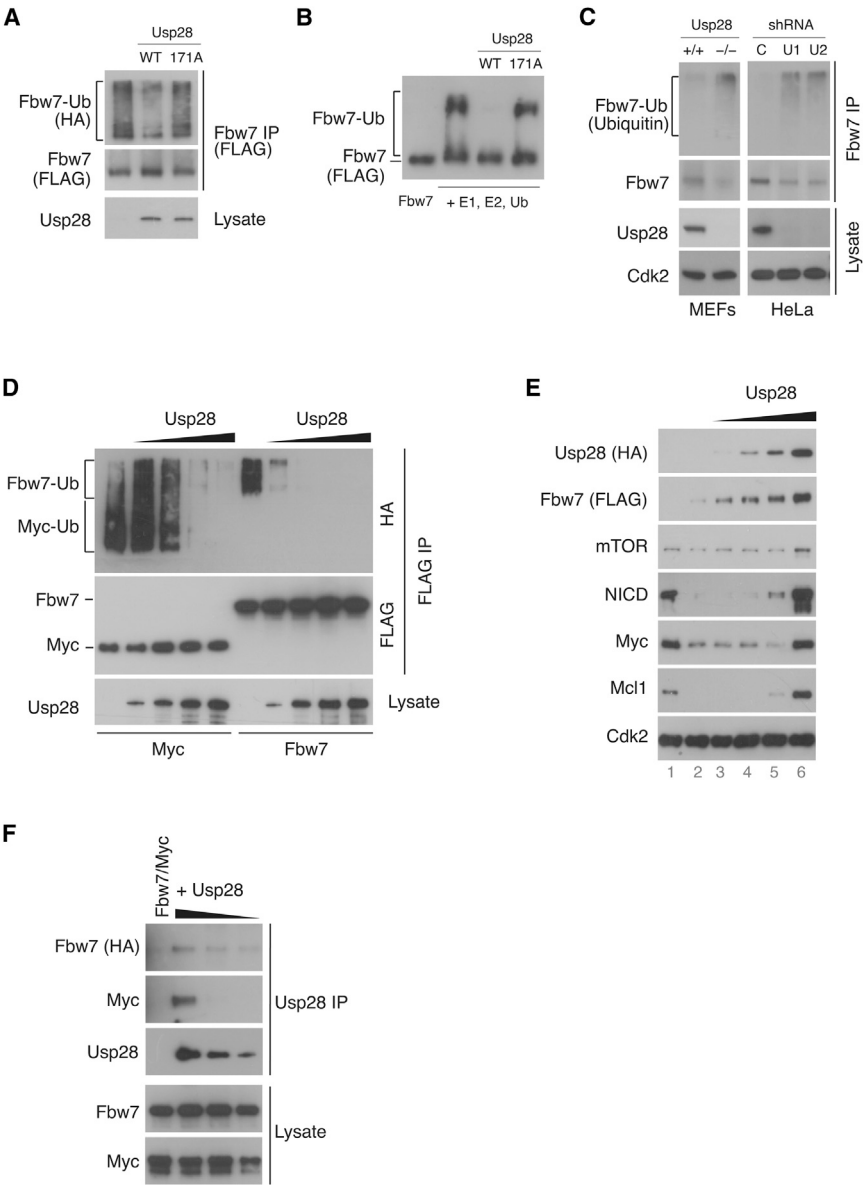

Figure 4. Usp28 Stabilizes Fbw7 and Its Substrates at Distinct Abundance Thresholds

(A) HeLa cells were cotransfected with FLAG-Fbw7, HA-tagged Ub, and Usp28. Ubiquitinated Fbw7 was recovered by immunoprecipitation and analyzed by immunoblotting with indicated antibodies. A representative of three experiments is shown.

(B) In vitro deubiquitination reactions were performed with immunopurified SCF(FLAG-Fbw7), recombinant E1, E2, and ubiquitin and immunopurified HA-tagged WT or C171A mutant Usp28.

(C) *Usp28*$^{+/+}$ and *Usp28*$^{-/-}$ MEFs, and HeLa cells, expressing control- (C) or Usp28-targeting shRNAs (U1, U2) were lysed and immunoprecipitated by with Fbw7 antibody followed by immunoblotting with antibodies to Fbw7 and ubiquitin. A representative of three experiments is shown.

(D) HeLa cells were transfected with FLAG-tagged Fbw7 or Myc, HA-tagged ubiquitin and increasing amounts of Usp28. Ubiquitinated Fbw7 and Myc were recovered by immunoprecipitation with FLAG antibodies and analyzed by anti-HA immunoblots for ubiquitin and anti-FLAG for Myc and Fbw7.

(E) Immunoblot analysis of HeLa cells cotransfected with Fbw7 substrates, without or with Fbw7 and increasing amounts of Usp28. See also Figure S4D.

(F) Anti-FLAG immunoprecipitation was performed from lysates of HeLa cells transfected with HA-tagged Myc and Fbw7 and FLAG-tagged Usp28. Precipitated protein complexes were analyzed by immunoblotting. A representative of three experiments is shown.

Usp28 and partially recovered in cells with a more efficient knockdown (Figure S4C).

Overexpression of Usp28 also stabilized endogenous Fbw7 and its substrates in HCT116 and HeLa cells (Figure S4D; data not shown). In HCT116 cells, consistent with higher sensitivity of Fbw7 to Usp28, Fbw7 was maximally upregulated already at the lowest amount of ectopic Usp28, whereas Fbw7 substrate levels increased gradually with increasing amounts of Usp28. Deletion of Fbw7 upregulated basal substrate levels, but strongly diminished (cyclin E) or eliminated (Myc, Jun, mTOR) the stabilizing effect of ectopic Usp28, in agreement with our previous findings (Figure S4D) (Popov et al., 2007a).

To compare the ability of Usp28 to recruit Fbw7 versus an Fbw7 substrate, we cotransfected HeLa cells with Fbw7, Myc, and different amounts of Usp28 and analyzed immunoprecipitated Usp28 complexes. Usp28 recruited Fbw7 at all levels but bound Myc only at the highest level of expression (Figure 4F). This result suggests that Usp28 preferentially stabilizes Fbw7 due to more efficient binding and is consistent with the idea that Fbw7 targets Usp28 to its substrates.

We concluded that stabilization of Fbw7 requires low levels of Usp28, whereas Fbw7 substrate stabilization occurs at higher levels, explaining the biphasic regulation of Fbw7 substrates in knockout cells.

Monoallelic Loss of *Usp28* Deregulates Transcription and Cell Proliferation Downstream of Fbw7

Many of the Fbw7/Usp28 substrates are transcription factors and are strongly deregulated in *Usp28*-deficient MEFs and murine tissues. To measure the transcriptional response to *Usp28* loss, we performed RNA sequencing using three preparations of immortalized MEFs with different levels of *Usp28*. Initial analysis of relative expression of all genes revealed an unexpected pattern of regulation with a stronger effect in *Usp28*$^{+/-}$ MEFs compared to the *Usp28*$^{-/-}$ cells (Figure S5A). For a more

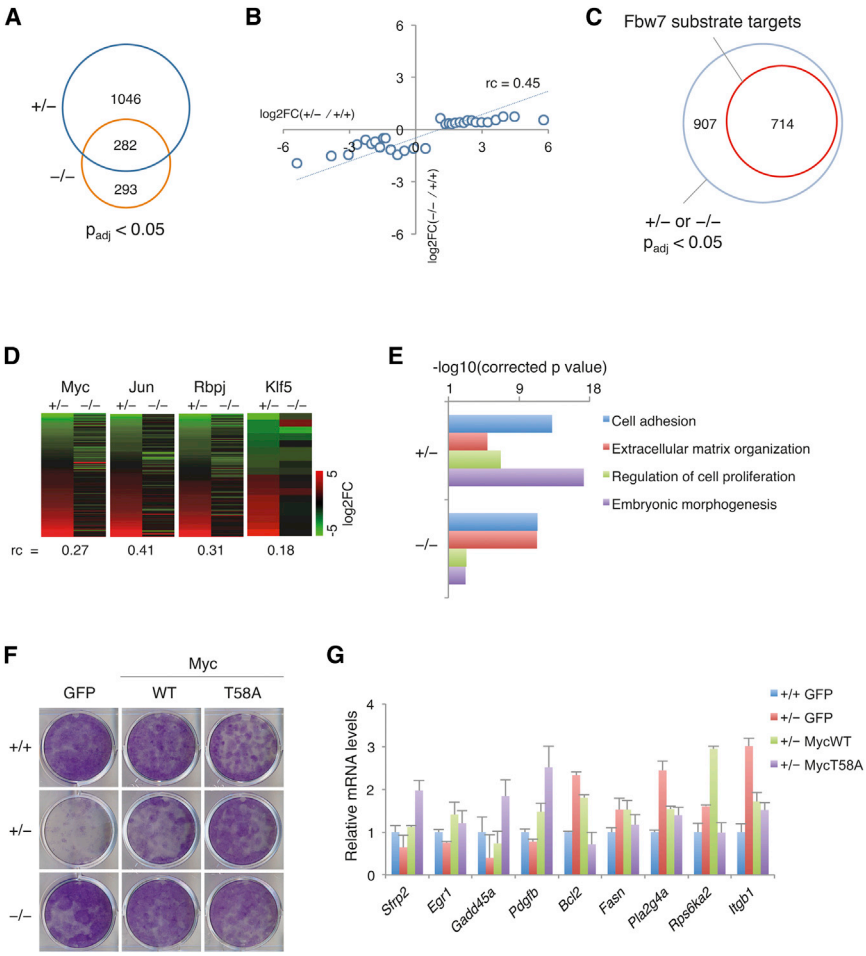

Figure 5. Monoallelic Loss of *Usp28* Deregulates Transcription and Cell Proliferation Downstream of Fbw7

(A) Venn diagram shows number of common and unique genes significantly deregulated (p_{adj} for $log_2FC < 0.05$) in either *Usp28*$^{+/-}$ or *Usp28*$^{-/-}$ MEFs. See also Figure S5A.

(B) Regulation for significantly deregulated genes in *Usp28*$^{+/-}$ or *Usp28*$^{-/-}$ MEFs (defined in A). Each dot corresponds to a median of log_2FC values for 50 genes, sorted by the regulation in *Usp28*$^{+/-}$ MEFs. To fairly display the majority of deregulated genes, the plot excludes outliers.

(C) Direct target genes of Fbw7 substrates: Myc, Jun, p63, Srepb1, Srebp2, Rbpj/NICD, Myb, and Klf5, together account for 714 of the total of 1,621 significantly deregulated genes. See also Figure S5C.

(D) Heatmaps visualize deregulation of the direct targets of Fbw7 substrates in *Usp28*$^{+/-}$ and *Usp28*$^{-/-}$ MEFs. The rc values characterize relative log_2FC regulation for target genes of individual transcription factors in *Usp28*$^{+/-}$ versus *Usp28*$^{-/-}$ MEFs; compare to the rc value for all significantly deregulated genes shown in (B).

(E) Gene ontology analysis using DAVID knowledgebase identifies biological processes enriched among genes deregulated in *Usp28*$^{+/-}$ and *Usp28*$^{-/-}$ MEFs.

(F) MEFs were transduced with retroviruses expressing wild-type or the T58A mutant Myc, and selected cell pools were analyzed for colony formation. A representative of three independent experiments is shown.

(G) qRT-PCR analysis of gene expression in *Usp28*$^{+/-}$ MEFs transduced with wild-type or the T58A mutant Myc compared to GFP-transduced *Usp28*$^{+/+}$ MEFs. Error bars show SD.

consistent gene representation, we narrowed subsequent analysis to genes, which were significantly deregulated in all biological replicates (p_{adj} for log_2FC in either genotype <0.05), and validated regulation of several genes using quantitative RT-PCR (qRT-PCR) (Figure S5B).

The number of deregulated genes was 1,328 for the *Usp28*$^{+/-}$ MEFs and only 575 for the *Usp28*$^{-/-}$ MEFs (Figure 5A). To visualize and compare gene regulation in these cells, we binned the genes according to the regulation in the *Usp28*$^{+/-}$ MEFs and plotted the median values of the bins (Figure 5B). As in the unfiltered data set, gene expression was affected much stronger in the *Usp28*$^{+/-}$ MEFs compared to *Usp28*$^{-/-}$ MEFs (regression coefficient rc = 0.45, versus an expected rc > 1).

This pattern of gene regulation paralleled observed effects on protein levels of Fbw7 substrates, raising the possibility that the latter account for most of transcriptional changes in *Usp28* knockout cells. Indeed, comparison of deregulated transcripts to the chromatin immunoprecipitation-based data sets using CHEA database revealed significant enrichment of direct targets of most published Fbw7 substrates, including Myc, Jun, Rbpj/NICD, Klf5, Myb, and p63 (Figure S5C) (Lachmann et al., 2010). Together, Fbw7 substrates accounted for 714 genes, approximately half of the deregulated transcriptome (Figures 5C and S5C). For the transcriptional targets of individual Fbw7 substrates, the difference in regulation in *Usp28*$^{+/-}$ versus *Usp28*$^{-/-}$ was even stronger than for all of the deregulated genes (Figure 5D, note the rc values of 0.27 for Myc, 0.31 for Rbpj/NICD, and 0.18 for Klf5); this effect was especially apparent for the activated transcripts (putative Fbw7 substrate-repressed target genes), which remained essentially unaffected in the *Usp28*$^{-/-}$ MEFs relative to the wild-type MEFs.

Functional annotation of the deregulated transcriptome using DAVID knowledgebase revealed distinct patterns of representation for different biological processes between *Usp28*$^{+/-}$ and *Usp28*$^{-/-}$ MEFs (Sherman et al., 2007). For example, deregulation of transcripts associated with extracellular matrix organization was more apparent in the *Usp28*$^{-/-}$ cells, suggesting that these genes are regulated by Usp28 independently of Fbw7 (Figure 5E). Genes, associated with cell adhesion were enriched equivalently in *Usp28*$^{+/-}$ and *Usp28*$^{-/-}$ MEFs, indicating that Usp28 may be haploinsufficient for regulation of certain biological pathways (Figure 5E). In contrast, genes implicated in cell proliferation and embryonic morphogenesis were regulated significantly stronger in the *Usp28*$^{+/-}$ cells, arguing that these processes are regulated by Fbw7 substrates. In agreement with this notion, ectopic expression of Fbw7-resistant Myc

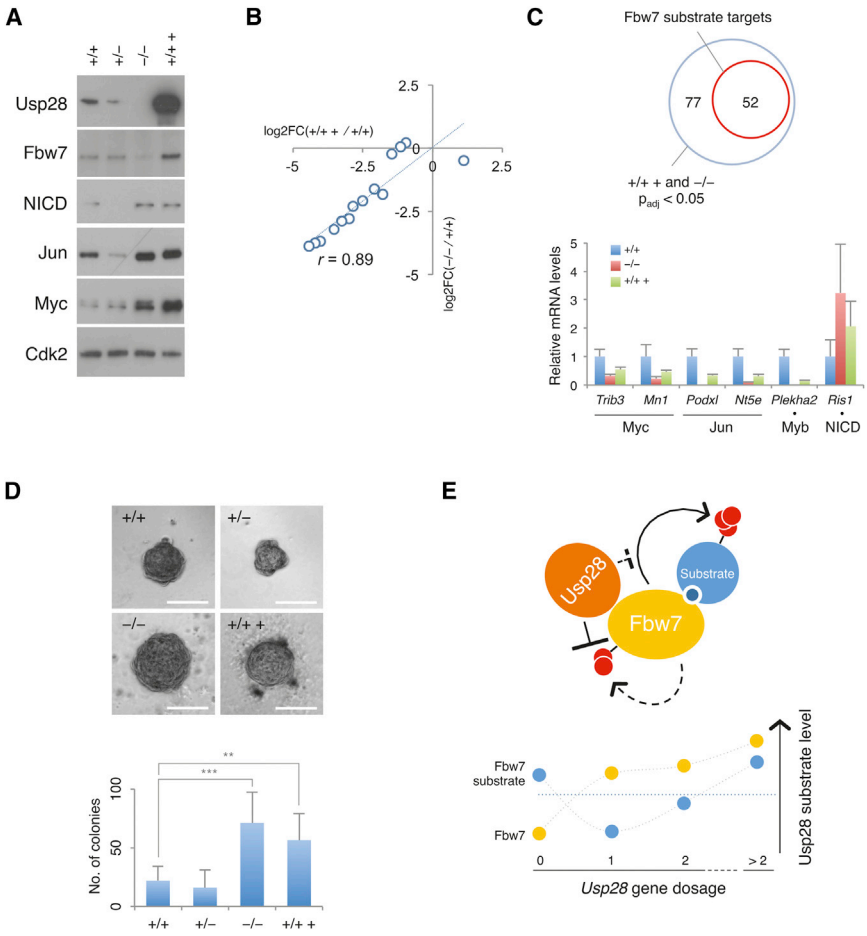

Figure 6. Complete Loss or Overexpression of *Usp28* Promote Cell Transformation

(A) Fbw7 and Fbw7 substrate levels in HRasG12V-expressing MEFs with different genetic status of *Usp28*. See also Figure S6.

(B) Scatterplot visualizes regulation of genes, significantly deregulated in *Usp28*-overexpressing MEFs (+/+ +) relative to changes in *Usp28*$^{-/-}$ (–/–). Each dot represents a median $\log_2$FC value for a bin of ten genes, sorted according to the regulation in *Usp28*-overexpressing cells.

(C) The diagram shows representation of Fbw7 substrate targets within genes coregulated in transformed Usp28-overexpressing and Usp28-null cells. qRT-PCR validates coregulation of targets genes of Myc, Jun, Myb, and NICD, by Usp28 loss and overexpression. Error bars show SD.

(D) Representative colonies of Ras-transformed MEFs of the indicated genotypes grown in soft agar. Colony counts for three biological replicates each from three independently transduced MEF pools are shown in the graph below. Error bars show SD of all biological replicates; **p < 0.01 and *** p < 0.001 were as determined by Student's t test.

(E) Model for dual regulation of Fbw7 substrate by Usp28. Usp28 antagonizes both substrate targeting and autocatalytic ubiquitination by Fbw7 but preferentially deubiquitinates Fbw7. Lower panel shows the observed effect of different dosage of *Usp28* on the abundance of Fbw7 and its substrates. Fbw7 stability requires minimal amount of Usp28 and increases with Usp28 levels, whereas Fbw7 substrates are regulated in a biphasic manner. Both loss and overexpression of Usp28 raise Fbw7 substrate abundance above the homeostatic boundary (blue dotted line) and promote cell transformation.

mutant (T58A) and to a lesser extent of wild-type Myc in *Usp28*$^{+/-}$ MEFs enabled efficient proliferation and rescued expression of multiple established Myc target genes (Figures 5F and 5G).

Thus, a significant fraction of the MEF transcriptome shows a biphasic response to loss of *Usp28*, supporting the notion that Usp28-dependent transcriptional programs are largely mediated by Fbw7 substrates. Among these, the proliferative program is likely to be controlled by Usp28 directly via the Fbw7-Myc pathway.

Biallelic Loss or Overexpression of *Usp28* Promote Fbw7 Substrate Stabilization and Oncogenic Transformation

Fbw7 substrates, such as Myc and Jun, promote cell transformation in vitro and drive tumorigenesis in mouse models. In *Usp28*$^{-/-}$ MEFs Fbw7 substrates accumulate due to strong destabilization of Fbw7. On the other hand, in transient assays, Usp28 overexpression stabilizes both Fbw7 and its substrates. To directly compare how these two conditions affect levels and activity of Fbw7 substrates in the context of oncogenic signaling, we stably expressed an activated Hras variant, G12V, in *Usp28*$^{-/-}$, *Usp28*$^{+/-}$ or wild-type MEFs with or without ectopic Usp28.

Expression of Ras in *Usp28*$^{+/-}$ MEFs rescued levels of Myc, but not of NICD, Jun, Mcl1, or mTOR, possibly due to the effects of Ras on kinases, which specifically regulate Myc phosphorylation at CPD (Figure 6A; data not shown) (Sears et al., 2000). Intriguingly, both ectopic expression of Usp28 in wild-type MEFs (+/+ +) and complete knockout of *Usp28* (–/–) strongly and equivalently increased levels of Myc, Jun, and Notch (Figure 6A). Endogenous Fbw7 was downregulated in the *Usp28*$^{-/-}$ MEFs but sharply upregulated in cells with ectopic Usp28, demonstrating that overexpression of Usp28 suffices to simultaneously stabilize Fbw7 and its substrates (Figure 6A). Depletion of Fbw7 in Usp28-overexpressing and *Usp28*$^{-/-}$ MEFs did not strongly affect Fbw7 substrate abundance, consistent with the idea that Fbw7 function is attenuated in these cells by enhanced deubiquitination or autocatalytic ubiquitin transfer (Figure S6).

Next, we sequenced RNA from transformed MEFs with different status of Usp28 to determine whether equivalent accumulation of Fbw7 substrates in Usp28-null and Usp28-overexpressing cells results in similar downstream transcriptional responses. Overexpression of Usp28 significantly deregulated 155 genes (padj < 0.05), most of which were repressed. To compare the regulation of these genes in Usp28-overexpressing (+/+ +) and *Usp28*$^{-/-}$ (–/–) cells, we binned the genes according

to the regulation in Usp28-overexpressing cells and plotted the median values of the bins. Strikingly, the direction and extent of regulation of these genes in the *Usp28*$^{-/-}$ MEFs very closely matched that in *Usp28*-overexpressing cells (Figure 6B). CHEA analysis revealed significant enrichment of transcriptional targets of Myc and Jun (Figure 6F, $p = 3.4 \times 10^{-5}$ for Myc; $p = 1.2 \times 10^{-4}$ for Jun) and also identified targets of NICD, Myb, and KLF5 within this gene set (Figure 6C; data not shown). qPCR experiments confirmed that multiple cancer-relevant transcriptional targets of Fbw7 substrates were similarly regulated by overexpression and complete loss of Usp28 (Figure 6C; data not shown).

We then measured the ability of Ras-expressing MEFs with different levels of Usp28 to grow in an anchorage-independent manner, a defining feature of transformed cells in vitro. Ras-expressing *Usp28*$^{+/-}$ MEFs showed wild-type colony-forming ability in soft agar, possibly due to the enhanced levels of Myc in these cells (Figure 6D). Strikingly, both the complete loss and the ectopic expression of Usp28 strongly stimulated anchorage-independent growth. This effect correlated with equivalent upregulation of Fbw7 substrates in these cells, suggesting that loss and overexpression of Usp28 promote oncogenic transformation via stabilization of Fbw7 substrates (Figures 6A and 6D).

In summary, we propose that Usp28 exerts a dual effect on Fbw7 activity by antagonizing both substrate-directed and autocatalytic ubiquitination of Fbw7 (Figure 6E, top panel). Usp28 preferentially deubiquitinates Fbw7 and at intermediate levels maintains stable Fbw7 but does not allow excessive Fbw7 substrate stabilization. Either complete loss or overexpression of Usp28 stabilize Fbw7 substrates and promote malignant transformation in the context of cooperating oncogenic events (Figure 6E, lower panel).

DISCUSSION

Here, we have used knockout mice to analyze the role of Usp28 in Fbw7-mediated substrate degradation in vivo. Monoalleilc loss of Usp28, as expected, reduced levels of Fbw7 substrates across all the examined tissues. Strikingly, complete knockout of Usp28 produced tissue-specific effects; in most of the tested tissues (e.g., lung, pancreas, and liver) and MEFs, Fbw7 substrates accumulate due to the destabilization of Fbw7. In contrast, in the intestine and cerebellum, complete loss of Usp28 did not reduce Fbw7 levels but downregulated Fbw7 substrates.

Mechanistic analysis revealed that this biphasic response to Usp28 loss is due to preferential recruitment and deubiquitination of Fbw7, compared to Fbw7 substrates, by Usp28. Consequently, half of the normal dose of Usp28 (in the *Usp28*$^{+/-}$ cells) is adequate to maintain stable Fbw7 but is not sufficient to antagonize Fbw7-mediated substrate degradation. In contrast, complete absence of Usp28 triggers autocatalytic turnover of Fbw7 and leads to Fbw7 substrate stabilization.

The most likely explanation for such nonlinear pattern of regulation is that Fbw7 substrates are recruited to Usp28 via Fbw7 and therefore their interaction with Usp28 is less efficient (Figure 4F) (Popov et al., 2007a). Similar relationship has been described in the Mdm2-HAUSP-p53 circuit, in which higher affinity of HAUSP for Mdm2 due to an extended binding interface results in the biphasic regulation of p53 (Li et al., 2004; Hu et al., 2006).

A possible reason for the tissue-specific response to complete Usp28 loss is that autocatalytic ubiquitination by Fbw7 is modulated by upstream signaling, which differs in individual tissues. In agreement with this idea, autocatalytic ubiquitination by Fbw7 in *Usp28*$^{-/-}$ MEFs required peptidyl-prolyl isomerase Pin1, which switches Fbw7 from substrate targeting to autocatalytic "mode" (Figures 3F–3H) (Min et al., 2012). Chemical inhibition of Pin1 or mutation of Fbw7 at Ser205, a residue recognized by Pin1, stabilized Fbw7 and promoted substrate degradation in *Usp28*$^{-/-}$ MEFs (Figures 3F–3H). In line with this, relative levels of Pin1 in tissues correlated with Fbw7 substrate levels; they decreased with loss of Usp28 in the intestine but accumulated in the lung (Figure S3F). Therefore, we propose that tissue-specific signals that modulate the expression or activity of Pin1, a Ser205-targeting kinase, or similarly acting enzymes, determine the outcome of Usp28 loss on Fbw7 substrate levels.

A striking observation in *Usp28* knockout mice is that although several critical substrates of Fbw7 (e.g., Jun, Myc, and cyclin E) are strongly downregulated, tissue architecture and homeostasis are essentially normal. We suggest that destabilization of additional antiproliferative substrates of Fbw7, such as JunB, CEBPα, and p63, may relieve the requirement for explicit proliferative signaling in vivo and allow adequate homeostasis in the absence of Usp28 (Bengoechea-Alonso and Ericsson, 2010; Galli et al., 2010; Pérez-Benavente et al., 2013). On the other hand, downregulation of Fbw7, induced by *Usp28* loss is either not sufficient to promote embryonic lethality, associated with *Fbxw7* knockout, or does not occur in lineages, in which Fbw7 is essential during development (Tsunematsu et al., 2004).

A key biological question reemerging from our analysis is what the advantage is of coupling opposing ubiquitin de/conjugating activities in one functional unit. Such ubiquitin ligase-DUB pairs are widespread in signaling networks, exemplified by recent analysis of APC/C(Cdh1)-Usp37, Itch-CYLD, and LUBAC-OTULIN complexes (Huang et al., 2011; Ahmed et al., 2011; Keusekotten et al., 2013). Discovery of an analog of the Fbw7-Usp28 complex in *Drosophila* demonstrates that such complexes represent an evolutionary conserved regulatory paradigm (Li et al., 2013). However, the molecular logic for integrating these antagonistic functions often remains elusive.

In some situations, distinct specificity of the DUB and the ligase for different ubiquitin chain linkages allows chain editing and repurposing of the modified substrate (Ahmed et al., 2011). In others, coupling two antagonistic activities may allow a rapid and transient change in substrate abundance in response to upstream signals, which mediate complex assembly or control activity of one of the enzymes (Popov et al., 2007b; Huang et al., 2011).

In case of the Fbw7-Usp28 complex, we suggest that wiring control of the ligase and its substrates to a single DUB ensures that stabilization of proto-oncoproteins during homeostatic processes occurs only transiently. Because an event that activates Usp28 will stabilize Fbw7 substrates but also Fbw7, such design efficiently suppresses prolonged proliferative or survival signaling. Preferential targeting of Fbw7 by Usp28 shifts the

default activity of this system toward Fbw7 substrate ubiquitination and provides a mechanism to maintain physiological levels of multiple proto-oncoproteins.

Loss or overexpression of Usp28 disrupts this balance and leads to Fbw7 substrate accumulation (either via destabilization of Fbw7 or via stabilization of both Fbw7 and its substrates) and both conditions promote Ras-dependent cell transformation. Interestingly, genomic studies reveal that both deletions and overexpression of *USP28* occur in human cancer. Consistent with tissue-specific effects of Usp28 on Fbw7 described here, *USP28* is amplified or overexpressed in colorectal and ovarian cancers, whereas prostate, breast, and skin cancers harbor deletions in *USP28* (Forbes et al., 2008; Cerami et al., 2012; Diefenbacher et al., 2014). It will be important to establish whether these opposite genetic alterations of *USP28* in human cancer also equivalently promote tumorigenesis via stabilization of Fbw7 substrates, potentially making Usp28 a context-dependent tumor promoter or suppressor.

EXPERIMENTAL PROCEDURES

Mice

Generation of the $Usp28^{fl/fl}$ mice has been described in detail (Diefenbacher et al., 2014). Briefly, loxP sites were introduced in the intronic sequences flanking exons 4 and 5 of the *Usp28* gene. Cre recombinase-mediated excision results in the removal of sequences encoding the catalytic domain and in a frameshift in the downstream sequence. Constitutive knockout *Usp28* mice were obtained by crossing $Usp28^{fl/fl}$ with *Zp3-cre* mice (de Vries et al., 2000). All tissue samples were collected from 8-week-old animals. Animal experiments were carried out according to German law and were approved by the ethics committee (Tierschutzkommission der Regierung von Unterfranken).

Cell Culture

Mouse embryonic fibroblasts (MEFs) were isolated from E13.5 embryos and cultured in DMEM (Sigma) supplemented with 10% FBS (Biochrom) and 1% penicillin/streptomycin. Primary MEF cultures were immortalized by transduction with retroviruses encoding shRNA against *Arf* conferring puromycin or blasticidin resistance. Colony formation assays, anchorage-independent growth, and inhibitor treatment are detailed in Supplemental Experimental Procedures.

Immunoblotting

Tissue extracts were prepared by homogenization in RIPA buffer. Whole-cell extracts from cultured cells were obtained by boiling cell suspensions in SDS sample buffer. For detection of endogenous Fbw7, cells or tissue samples were lysed in RIPA buffer and immunoprecipitated with Fbw7 antibodies, as detailed in Supplemental Experimental Procedures. SDS-PAGE and immunoblotting were performed as described previously using antibodies listed in Supplemental Experimental Procedures (Popov et al., 2010).

Immunoprecipitation and In Vivo Deubiquitination

For deubiquitination assays, HeLa cells were cotransfected with FLAG-tagged Myc and Fbw7, HA-tagged ubiquitin, and increasing amounts of HA-tagged Usp28. For immunoprecipitations, HeLa cells were cotransfected with FLAG-tagged Usp28, and HA-tagged Fbw7 and Myc. Pull-downs were performed with anti-FLAG antibodies (Sigma) as described previously (Popov et al., 2010).

In Vitro Ubiquitination Assays

Reactions were performed with immunopurified SCF complexes (via FLAG-tagged Fbw7), immunopurified HA-tagged Usp28, and recombinant polyhistidine-tagged Ube1, UbcH3, and ubiquitin (Boston Biochem). See also Supplemental Experimental Procedures.

RNA Sequencing

For the immortal MEFs, three independent preparations were plated at 500,000 cells per 10 cm dish; the transformed MEFs were plated in duplicates at 300,000 cells per 10 cm dish. After 24 hr, total RNA was isolated with the RNeasy Mini Kit (QIAGEN) including on-column DNA digestion. The quality and integrity of the RNA was determined with an Experion Automated Electrophoresis System (Bio-Rad). The poly(A)+with Sera-Mag Magnetic Oligo(dT) Microparticles (Thermo Scientific) and used for library preparation with NEBNext mRNA Library Prep Master Mix set for Illumina (immortal MEFs) or NEBNext UltraTM RNA Library Prep Kit for Illumina (transformed MEFs). The resulting library was sequenced with the Illumina Genome Analyzer IIx according to the manufacturers' instructions.

ACCESSION NUMBERS

The sequencing data have been submitted to the GEO repository under accession number GSE59354.

SUPPLEMENTAL INFORMATION

Supplemental Information includes Supplemental Experimental Procedures and six figures and can be found with this article online at http://dx.doi.org/10.1016/j.celrep.2014.09.057.

ACKNOWLEDGMENTS

This work was supported by grants from the German Science Foundation (DFG Research grant PO1458-3/1 to N.P. and ME222/12-1 to M.E.), from the Wilhelm-Sander-Stiftung (to M.E.) and by an institutional grant of the Deutsche Krebshilfe. We thank Kseniya Popova, Angela Grün, Renate Metz, and Barbara Bauer for expert technical assistance, Björn von Eyss for help with statistical analysis, Alex Buchberger for anti-Rbx1 antibody, Thomas Westbrook for pInducer20 vector, and M.E. lab members for critical reading of the manuscript.

Received: March 21, 2014
Revised: September 11, 2014
Accepted: September 28, 2014
Published: October 30, 2014

REFERENCES

Ahmed, N., Zeng, M., Sinha, I., Polin, L., Wei, W.-Z., Rathinam, C., Flavell, R., Massoumi, R., and Venuprasad, K. (2011). The E3 ligase Itch and deubiquitinase Cyld act together to regulate Tak1 and inflammation. Nat. Immunol. *12*, 1176–1183.

Akhoondi, S., Sun, D., von der Lehr, N., Apostolidou, S., Klotz, K., Maljukova, A., Cepeda, D., Fiegl, H., Dafou, D., Marth, C., et al. (2007). FBXW7/hCDC4 is a general tumor suppressor in human cancer. Cancer Res. *67*, 9006–9012.

Bassermann, F., Frescas, D., Guardavaccaro, D., Busino, L., Peschiaroli, A., and Pagano, M. (2008). The Cdc14B-Cdh1-Plk1 axis controls the G2 DNA-damage-response checkpoint. Cell *134*, 256–267.

Bengoechea-Alonso, M.T., and Ericsson, J. (2010). The ubiquitin ligase Fbxw7 controls adipocyte differentiation by targeting C/EBPalpha for degradation. Proc. Natl. Acad. Sci. USA *107*, 11817–11822.

Cerami, E., Gao, J., Dogrusoz, U., Gross, B.E., Sumer, S.O., Aksoy, B.A., Jacobsen, A., Byrne, C.J., Heuer, M.L., Larsson, E., et al. (2012). The cBio cancer genomics portal: an open platform for exploring multidimensional cancer genomics data. Cancer Discov *2*, 401–404.

Chen, B.B., Glasser, J.R., Coon, T.A., Zou, C., Miller, H.L., Fenton, M., McDyer, J.F., Boyiadzis, M., and Mallampalli, R.K. (2012). F-box protein FBXL2 targets cyclin D2 for ubiquitination and degradation to inhibit leukemic cell proliferation. Blood *119*, 3132–3141.

de Vries, W.N., Binns, L.T., Fancher, K.S., Dean, J., Moore, R., Kemler, R., and Knowles, B.B. (2000). Expression of Cre recombinase in mouse oocytes: a means to study maternal effect genes. Genesis *26*, 110–112.

Diefenbacher, M.E., Popov, N., Blake, S.M., Schülein-Völk, C., Nye, E., Spencer-Dene, B., Jaenicke, L.A., Eilers, M., and Behrens, A. (2014). The deubiquitinase USP28 controls intestinal homeostasis and promotes colorectal cancer. J. Clin. Invest. *124*, 3407–3418.

Durgan, J., and Parker, P.J. (2010). Regulation of the tumour suppressor Fbw7α by PKC-dependent phosphorylation and cancer-associated mutations. Biochem. J. *432*, 77–87.

Flügel, D., Görlach, A., and Kietzmann, T. (2012). GSK-3β regulates cell growth, migration, and angiogenesis via Fbw7 and USP28-dependent degradation of HIF-1α. Blood *119*, 1292–1301.

Forbes, S.A., Bhamra, G., Bamford, S., Dawson, E., Kok, C., Clements, J., Menzies, A., Teague, J.W., Futreal, P.A., and Stratton, M.R. (2008). The catalogue of somatic mutations in cancer (COSMIC). Curr. Protoc. Hum. Genet. *10*, 10.11.

Galli, F., Rossi, M., D'Alessandra, Y., De Simone, M., Lopardo, T., Haupt, Y., Alsheich-Bartok, O., Anzi, S., Shaulian, E., Calabrò, V., et al. (2010). MDM2 and Fbw7 cooperate to induce p63 protein degradation following DNA damage and cell differentiation. J. Cell Sci. *123*, 2423–2433.

Hoeller, D., and Dikic, I. (2009). Targeting the ubiquitin system in cancer therapy. Nature *458*, 438–444.

Hu, M., Gu, L., Li, M., Jeffrey, P.D., Gu, W., and Shi, Y. (2006). Structural basis of competitive recognition of p53 and MDM2 by HAUSP/USP7: implications for the regulation of the p53-MDM2 pathway. PLoS Biol. *4*, e27.

Huang, X., Summers, M.K., Pham, V., Lill, J.R., Liu, J., Lee, G., Kirkpatrick, D.S., Jackson, P.K., Fang, G., and Dixit, V.M. (2011). Deubiquitinase USP37 is activated by CDK2 to antagonize APC(CDH1) and promote S phase entry. Mol. Cell *42*, 511–523.

Keusekotten, K., Elliott, P.R., Glockner, L., Fiil, B.K., Damgaard, R.B., Kulathu, Y., Wauer, T., Hospenthal, M.K., Gyrd-Hansen, M., Krappmann, D., et al. (2013). OTULIN antagonizes LUBAC signaling by specifically hydrolyzing Met1-linked polyubiquitin. Cell *153*, 1312–1326.

Knobel, P.A., Belotserkovskaya, R., Galanty, Y., Schmidt, C.K., Jackson, S.P., and Stracker, T.H. (2014). USP28 is recruited to sites of DNA damage by the tandem BRCT domains of 53BP1 but plays a minor role in double-strand break metabolism. Mol. Cell. Biol. *34*, 2062–2074.

Lachmann, A., Xu, H., Krishnan, J., Berger, S.I., Mazloom, A.R., and Ma'ayan, A. (2010). ChEA: transcription factor regulation inferred from integrating genome-wide ChIP-X experiments. Bioinformatics *26*, 2438–2444.

Li, M., Brooks, C.L., Kon, N., and Gu, W. (2004). A dynamic role of HAUSP in the p53-Mdm2 pathway. Mol. Cell *13*, 879–886.

Li, L., Anderson, S., Secombe, J., and Eisenman, R.N. (2013). The Drosophila ubiquitin-specific protease Puffyeye regulates dMyc-mediated growth. Development *140*, 4776–4787.

Min, S.-H., Lau, A.W., Lee, T.H., Inuzuka, H., Wei, S., Huang, P., Shaik, S., Lee, D.Y., Finn, G., Balastik, M., et al. (2012). Negative regulation of the stability and tumor suppressor function of Fbw7 by the Pin1 prolyl isomerase. Mol. Cell *46*, 771–783.

Mo, J.-S., Ann, E.-J., Yoon, J.-H., Jung, J., Choi, Y.-H., Kim, H.-Y., Ahn, J.-S., Kim, S.-M., Kim, M.-Y., Hong, J.-A., et al. (2011). Serum- and glucocorticoid-inducible kinase 1 (SGK1) controls Notch1 signaling by downregulation of protein stability through Fbw7 ubiquitin ligase. J. Cell Sci. *124*, 100–112.

Penn, L.J., Brooks, M.W., Laufer, E.M., and Land, H. (1990). Negative autoregulation of c-myc transcription. EMBO J. *9*, 1113–1121.

Pérez-Benavente, B., García, J.L., Rodríguez, M.S., Pineda-Lucena, A., Piechaczyk, M., Font de Mora, J., and Farràs, R. (2013). GSK3-SCF(FBXW7) targets JunB for degradation in G2 to preserve chromatid cohesion before anaphase. Oncogene *32*, 2189–2199.

Popov, N., Wanzel, M., Madiredjo, M., Zhang, D., Beijersbergen, R., Bernards, R., Moll, R., Elledge, S.J., and Eilers, M. (2007a). The ubiquitin-specific protease USP28 is required for MYC stability. Nat. Cell Biol. *9*, 765–774.

Popov, N., Herold, S., Llamazares, M., Schülein, C., and Eilers, M. (2007b). Fbw7 and Usp28 regulate myc protein stability in response to DNA damage. Cell Cycle *6*, 2327–2331.

Popov, N., Schülein, C., Jaenicke, L.A., and Eilers, M. (2010). Ubiquitylation of the amino terminus of Myc by SCF(β-TrCP) antagonizes SCF(Fbw7)-mediated turnover. Nat. Cell Biol. *12*, 973–981.

Schülein, C., Eilers, M., and Popov, N. (2011). PI3K-dependent phosphorylation of Fbw7 modulates substrate degradation and activity. FEBS Lett. *585*, 2151–2157.

Sears, R., Nuckolls, F., Haura, E., Taya, Y., Tamai, K., and Nevins, J.R. (2000). Multiple Ras-dependent phosphorylation pathways regulate Myc protein stability. Genes Dev. *14*, 2501–2514.

Sherman, B.T., Huang, W., Tan, Q., Guo, Y., Bour, S., Liu, D., Stephens, R., Baseler, M.W., Lane, H.C., and Lempicki, R.A. (2007). DAVID Knowledgebase: a gene-centered database integrating heterogeneous gene annotation resources to facilitate high-throughput gene functional analysis. BMC Bioinformatics *8*, 426.

Tsunematsu, R., Nakayama, K., Oike, Y., Nishiyama, M., Ishida, N., Hatakeyama, S., Bessho, Y., Kageyama, R., Suda, T., and Nakayama, K.I. (2004). Mouse Fbw7/Sel-10/Cdc4 is required for notch degradation during vascular development. J. Biol. Chem. *279*, 9417–9423.

Vaites, L.P., Lee, E.K., Lian, Z., Barbash, O., Roy, D., Wasik, M., Klein-Szanto, A.J.P., Rustgi, A.K., and Diehl, J.A. (2011). The Fbx4 tumor suppressor regulates cyclin D1 accumulation and prevents neoplastic transformation. Mol. Cell. Biol. *31*, 4513–4523.

Wang, Z., Inuzuka, H., Zhong, J., Wan, L., Fukushima, H., Sarkar, F.H., and Wei, W. (2012). Tumor suppressor functions of FBW7 in cancer development and progression. FEBS Lett. *586*, 1409–1418.

Welcker, M., and Clurman, B.E. (2008). FBW7 ubiquitin ligase: a tumour suppressor at the crossroads of cell division, growth and differentiation. Nat. Rev. Cancer *8*, 83–93.

Welcker, M., Larimore, E.A., Swanger, J., Bengoechea-Alonso, M.T., Grim, J.E., Ericsson, J., Zheng, N., and Clurman, B.E. (2013). Fbw7 dimerization determines the specificity and robustness of substrate degradation. Genes Dev. *27*, 2531–2536.

Zhang, D., Zaugg, K., Mak, T.W., and Elledge, S.J. (2006). A role for the deubiquitinating enzyme USP28 in control of the DNA-damage response. Cell *126*, 529–542.